Journal of Neurochemistry
Lippincott Williams & Wilkins, Inc., Philadelphia

Increased Expression of Rat Synuclein in the Substantia Nigra Pars Compacta Identified by mRNA Differential Display in a Model of Developmental Target Injury

*Nikolai G. Kholodilov, *Michael Neystat, *Tinmarla F. Oo, *Steven E. Lo, *†Kristin E. Larsen, *†David Sulzer, and *‡Robert E. Burke

*Departments of *Neurology and ‡Pathology; and †Departments of Psychiatry and Neuroscience, New York State Psychiatric Institute, Columbia University, College of Physicians and Surgeons, New York, New York, U.S.A.*

Abstract: Human α-synuclein was identified on the basis of proteolytic fragments derived from senile plaques of Alzheimer's disease, and it is the locus of mutations in some familial forms of Parkinson's disease. Its normal function and whether it may play a direct role in neural degeneration remain unknown. To explore cellular responses to neural degeneration in the dopamine neurons of the substantia nigra, we have developed a rodent model of apoptotic death induced by developmental injury to their target, the striatum. We find by mRNA differential display that synuclein is up-regulated in this model, and thus it provides an opportunity to examine directly whether synuclein plays a role in the death of these neurons or, alternatively, in compensatory responses. Up-regulation of mRNA is associated with an increase in the number of neuronal profiles immunostained for synuclein protein. At a cellular level, synuclein is almost exclusively expressed in normal neurons, rather than apoptotic profiles. Synuclein is up-regulated throughout normal postnatal development of substantia nigra neurons, but it is not further up-regulated during periods of natural cell death. We conclude that up-regulation of synuclein in the target injury model is unlikely to mediate apoptotic death and propose that it may be due to a compensatory response in neurons destined to survive.
Key Words: Synuclein—Programmed cell death—Apoptosis—Substantia nigra—Dopaminergic neurons—Parkinson's disease.
J. Neurochem. **73,** 2586–2599 (1999).

Human α-synuclein was identified on the basis of proteolytic fragments derived from senile plaques of Alzheimer's disease. A 35-amino acid peptide fragment was named the non-Aβ component of amyloid, or NAC, and its 140-amino acid precursor was termed NACP (Ueda et al., 1993). NACP was also subsequently identified on the basis of its cross-reactivity with a monoclonal antibody that recognized phosphorylated tau protein (Jakes et al., 1994) and named α-synuclein, given its homology to synucleins that had been isolated from *Torpedo* electroplaques and identified in rat brain (Maroteaux et al., 1988; Maroteaux and Scheller, 1991). It is now recognized that in addition to human and rat α-synucleins, there are other members of a rapidly expanding family of synuclein-related proteins (for reviews, see Clayton and George, 1998; Lavedan, 1998). Nakajo et al. (1993, 1994) identified a 14-kDa protein, termed phosphoneuroprotein 14, that is homologous to α-synuclein and that, in rat brain, shares a similar distribution in axon terminals. Jakes et al. (1994) identified the 134-amino acid human homologue of this protein and termed it β-synuclein. More recently, another homologue has been isolated from breast cancer tissue (BCSG1) (Ji et al., 1997), and given its homology to α- and β-synucleins, the terminology γ-synuclein has been proposed (Lavedan et al., 1998). A phylogenetic analysis suggests that the first synuclein identified, that in *Torpedo*, by Maroteaux et al. (1988), is a member of this subfamily (Lavedan, 1998). A recently reported new member of the synuclein family, synoretin, identified on the basis of protein interaction with guanylate cyclase-activating protein, is also a member of this subfamily (Surguchov et al., 1999).

In relation to nomenclature, it is important to recognize that the proposed α, β, and γ designations are

Received June 25, 1999; revised manuscript received August 2, 1999; accepted August 2, 1999.

Address correspondence and reprint requests to Dr. R. E. Burke at Department of Neurology, Columbia University College of Physicians and Surgeons, Black Building, Room 308, 650 West 168th Street, New York, NY 10032, U.S.A.

The synuclein sequence in this study has been deposited with GenBank under accession number AF007758.

Abbreviations used: aRNA, antisense RNA; GAPDH, glyceraldehyde 3-phosphate dehydrogenase; HO2, hemoxygenase-2; IST, in situ transcription; NAC, non-Aβ component of amyloid; NACP, 140-amino acid precursor of non-Aβ component of amyloid; PBS, phosphate-buffered saline; PND, postnatal day; QA, quinolinic acid; SDS, sodium dodecyl sulfate; SN, substantia nigra; SNpc, substantia nigra pars compacta; SNpr, substantia nigra pars reticulata; SSC, saline–sodium citrate; TH, tyrosine hydroxylase; VMAT, vesicular monoamine transporter; VTA, ventral tegmental area.

distinct from the designations for three splice variants of rat α-synuclein, identified by Maroteaux and Scheller (1991) and termed synuclein 1, 2, and 3. Synuclein 1 encodes a 140-amino acid protein, identified by western analysis (Maroteaux and Scheller, 1991). Synuclein 2 and 3 encode predicted protein products of 149 and 42 amino acids, respectively; whether these predicted translation products are expressed is unknown (R. Scheller, personal communication). Thus, the protein product of the synuclein 1 mRNA splice variant is rat α-synuclein.

Little is known of the neurobiology of the synucleins, other than that they are localized to presynaptic terminals in both rat (Maroteaux et al., 1988) and human (Irizarry et al., 1996) brain and that a homologue in zebra finch, synelfin, is up-regulated during a period of neural plasticity related to song learning (George et al., 1995). The neurobiology of the synucleins has become of great interest in relation to neurodegenerative disease not only because the human form was identified in Alzheimer's brains, but also because mutations in α-synuclein have recently been identified in familial forms of Parkinson's disease (Polymeropoulos et al., 1997; Kruger et al., 1998). It is unknown whether synucleins may play a direct role in neural degeneration.

We have had an interest in the molecular events associated with neural degeneration in dopamine neurons of the substantia nigra (SN) pars compacta (SNpc), the neurons that degenerate in Parkinson's disease. One current hypothesis is that these neurons degenerate due to programmed cell death (Mochizuki et al., 1996; Tompkins et al., 1997). To explore this hypothesis, we have developed a model of induced programmed cell death in these neurons that is produced by axon-sparing destruction of the striatal target during development (Macaya et al., 1994). The exclusive occurrence of apoptosis in this model is confirmed by ultrastructural analysis, silver impregnation, and DNA end-labeling techniques and is identified within phenotypically defined dopamine neurons (Macaya et al., 1994). In this model, at most 25–30% of dopamine neurons die; the remainder survive into adulthood (Burke et al., 1992). The model thus provides a paradigm to identify not only the pathways mediating cell death, but also compensatory responses in the majority of dopamine neurons that survive. We have made the preliminary observation, based on an mRNA differential display technique, that rat synuclein 1 mRNA is up-regulated in this model (Kholodilov et al., 1997). Therefore, the model provides a unique opportunity to examine directly in dopamine neurons of the SNpc whether synuclein may play a role in apoptotic cell death or, alternatively, a role in cell responses related to viability or compensation, such as plasticity responses, as proposed for the avian homologue synelfin (George et al., 1995). We find that at a cellular level synuclein is expressed almost exclusively in morphologically normal neurons of the SNpc, rather than apoptotic profiles, and suggest that it is likely to play a role in viability or compensatory responses.

MATERIALS AND METHODS

Striatal lesions with quinolinic acid (QA)

Striatal QA lesions were performed as previously described (Macaya et al., 1994; Kelly and Burke, 1996) on postnatal day (PND) 7 or PND 12 rats; following induction of methoxyflurane (Metofane) anesthesia, a 28-gauge cannula was inserted into the striatum at 3.0 mm left of and 0.5 mm anterior to bregma, at a depth of 4.0 mm. QA (480 nmol/μl) in 0.1 *M* phosphate-buffered saline (PBS; pH 7.4) was infused by pump at 1.0 μl/2.0 min. PND 12 animals were used only in the immunohistochemical studies, to facilitate tissue processing. We have previously shown that the magnitude, distribution, and morphology of cell death in SN are identical between PND 7 and PND 14. This protocol has been approved by the Animal Care and Use Committee at Columbia-Presbyterian Medical Center.

mRNA differential display

SN tissues were obtained by microdissection. A 2.0-mm coronal section of the midbrain was taken, the dorsal portion was discarded, and left (experimental) and right (control) SNs were separated. Total RNA was isolated with a Qiagen RNAeasy kit and reverse-transcribed in three separate pools using anchored oligo(dT) primers with C, G, or A at the 3′ end. We then performed PCR on a subset of cDNAs within each pool using the same anchored primer end-labeled with [γ-^{32}P]ATP and one of 80 arbitrary primers (RNAimage kit; GenHunter) according to the manufacturer's instructions. The amplified products were then electrophoresed on 6% sequencing gels. To minimize the number of false-positives, four animals were analyzed separately, but in parallel, for each amplification at both 4 and 24 h poststriatal lesion. We accepted as positive only those bands that were differentially displayed in three or more animals for one or both times. We selected for analysis only those bands that were increased in their differential display on the experimental side because we sought mRNAs up-regulated by induction of cell death. After reamplification with appropriate pairs of primers, fragments were cloned in a pGEM-T vector (Promega). Plasmids from selected clones were isolated with a High Pure Plasmid Isolation Kit (Boehringer) and sequenced with an ABI PRIZM Dye Primer Cycle Sequencing Ready Reaction Kit followed by analysis on an ABI PRIZM 377 DNA Sequencer.

Comparative RT-PCR

Comparative RT-PCR of fragment 17 and synuclein 1 was performed using sequence-specific primers. For fragment 17 amplification, the forward primer was 17F (5′-TGCTGTGGATATTGTTGTGG-3′); the reverse primer was 17R (5′-AGGTGCGTAGTCTCATGCTC-3′). For synuclein 1 amplification, the forward primer was 5′-GTGTGGAGCAAAGATACATC-3′; the reverse primer was 17R. A partial sequence of the dopamine transporter, which is specifically localized to dopamine neurons, was used to control for symmetry of dissection, mRNA isolation, reverse transcription, and PCR. For the dopamine transporter, the forward primer was 5′-ACTGTAGTATGGCAGAGAAGGC-3′; the reverse primer was 5′-GAACCCACACAAGGTACTGG-3′. All PCR products were cloned in a pGEM-T vector and sequenced before use as templates for the generation of riboprobes. PCR was performed in 20 μl of solution containing 2 μl of 10× buffer (Promega), 2.5 m*M* $MgCl_2$, 300 μ*M* each deoxynucleotide triphosphate, 2 pmol of each primer, and 0.5 unit of *Taq* DNA polymerase (Promega). PCR was performed in a Hybaid OmnE

cycler according to the following program: 95°C for 5 min, followed by cycles of 94°C for 15 s, 51°C for 20 s, and 72°C for 30 s, and then a final elongation step at 74°C for 10 min. PCR products were analyzed by electrophoresis.

Northern analysis and in situ hybridization

For northern analysis SN was microdissected at various times following induction of lesions or at different postnatal times for the developmental studies. Total RNA was isolated with a Qiagen RNAeasy kit according to the manufacturer's instructions, and poly(A)$^+$ mRNA was isolated with a Qiagen Oligotex kit. For the striatal lesion studies, 0.6 μg of poly(A)$^+$ mRNA was electrophoresed in a 1.4% agarose gel and transferred to a Hybond membrane (Amersham). For the developmental studies, 10 μg of total RNA was electrophoresed. A riboprobe was created from the cloned fragment 17 with [α-^{33}P]UTP using a Promega riboprobe kit. BLAST analysis of the 354-bp fragment 17 revealed that it was not homologous to rat synuclein splice variant 2 or 3 or β- or γ-synuclein (see Results). Hybridization was performed in a solution containing 6× saline–sodium citrate (SSC), 5× Denhardt's solution, and 0.1% sodium dodecyl sulfate (SDS) at 65°C overnight. For in situ hybridization, rats were killed at 4 or 24 h after striatal lesion. Rats were perfused intracardially with chilled saline for 5 min, and the brains were then rapidly removed and frozen by immersion in 2-methylbutane on dry ice. The brains were then serially sectioned through the SN at 14 μm. Sections were thaw-mounted onto subbed slides and stored at −80°C until use. For hybridization, sections were fixed by immersion in 4% paraformaldehyde/0.1 *M* phosphate buffer (pH 7.1) for 5 min, rinsed twice in PBS, and delipidated by successive immersion in higher concentrations of ethanol and then chloroform. Sections were prehybridized at 40°C for 2 h with 1:1 formamide/prehybridization mix as previously described (Burke et al., 1994). Sections were then hybridized with 1:1 formamide/hybridization mix at 40°C overnight. Labeled riboprobe was added to a final activity of ~3,000 cpm/μl of the 1:1 formamide/hybridization solution. Following hybridizations, sections were washed in 2× SSC and then treated with RNase at 37°C for 45 min. They were then washed in 2× SSC for 60 min at 40°C, followed by immersion in 4 L of 0.1× SSC containing 0.05% sodium pyrophosphate and 14 m*M* 2-mercaptoethanol at 40°C for 3 h with gentle stirring. Sections remained in this wash at room temperature overnight. They were then dehydrated in ethanol, vacuum-dried, and apposed to x-ray film at −80°C for 3–4 weeks. ^{14}C standards embedded in plastic (Amersham) were enclosed in each cassette. Relative optical density measurements for the SNpc were made with a Loats Associates Inquiry image analysis system, as previously described (Burke et al., 1994).

Immunohistochemistry for synuclein 1, NAC, and tissue transglutaminase in tissue sections

For immunostaining of synuclein, eight animals underwent QA lesion at PND 12, and four each were killed at 4 and 24 h. Animals were perfused with 0.9% NaCl followed by 4% paraformaldehyde in 0.1 *M* phosphate buffer for 10 min. Brains were postfixed by immersion for 4 days and then cryoprotected in 20% sucrose. Brains were rapidly frozen in 2-methylbutane, and the SN was sectioned at 20 μm and processed free-floating.

Sections were first incubated with a rabbit anti-NACP(131–140) polyclonal antibody at 1:125 crude serum (Iwai et al., 1995) (kindly provided from the laboratory of Dr. T. Saitoh by Ms. M. Sundsmo) for 48 h at 4°C. This antibody recognizes the 10-amino acid C terminus of human NACP (EGYQDYEPEA), which is identical to the C-terminal sequence of α-synuclein in the rat (Maroteaux and Scheller, 1991). This sequence is unique to α-synuclein; it is not shared by the predicted protein products of the synuclein 2 and 3 splice variants or by β- or γ-synuclein. This antibody identifies a unique doublet band at 19 kDa in the cytosolic fraction of human and rat brain homogenates and has been used for immunohistochemical analysis of rat brain (Iwai et al., 1995). It does not cross-react with proteins at the lower expected molecular weights of β- or γ-synuclein. Following washes, sections were then incubated with protein A, biotinylated in this laboratory, at 1:100 for 60 min at room temperature. Sections were then incubated with avidin–biotin–peroxidase complexes (ABC kit; Vector) at 1:600 for 60 min. They were then incubated in diaminobenzidine and H_2O_2. Immunostaining for α-synuclein was confirmed by additional experiments with a mouse monoclonal antibody to rat synuclein(15–123) [anti-rSyn(15–123)] (Transduction Laboratories) at 1:200. This antibody recognizes a single band at the expected molecular size (19 kDa) in rat brain homogenates (authors' unpublished data).

For immunostaining of the NAC sequence, eight animals underwent QA lesion at PND 12, and four each were killed at 4 and 24 h and processed as described above, except postfixation time was only 3 h. Sections were stained using an anti-NAC rabbit polyclonal antibody at 1:200 (Iwai et al., 1995*a*,*b*) (also kindly provided by the laboratory of Dr. T. Saitoh) in 0.1 *M* PBS (pH 7.1) containing 0.5% bovine serum albumin and 0.1% Triton X-100 for 24 h. This antibody was raised to the N-terminal nine-amino acid sequence of a proteolytic fragment of human NAC (EQVTNVGGA), which is identical to the rat α-synuclein sequence from amino acid residues 61–69. This antibody recognizes the 35-amino acid NAC fragment (3.5 kDa), aggregates thereof, and Alzheimer's senile plaques (Iwai et al., 1995*a*,*b*). In addition, it stains Lewy bodies in Parkinson's disease brains (Arawaka et al., 1998). In our own experiments, this antibody on western blots also identifies in SN homogenates a band at the expected molecular mass for rat synuclein (Maroteaux and Scheller, 1991) and a second, previously unidentified band at 30 kDa. The portion of the protein recognized by the antibody corresponds to the main hydrophobic domain (Ueda et al., 1993).

Immunostaining for tissue transglutaminase was performed using a similar protocol, following incubation with rabbit anti-bovine transglutaminase at 1:200 (kindly provided by Dr. S. Hirose) in 0.1 *M* PBS (pH 7.1) containing 0.5% bovine serum albumin and 0.1% Triton X-100 for 24 h at 4°C. The number of synuclein-positive profiles in each SN was determined by scanning at a magnification of 600×. Three sections from representative anteroposterior planes [4.2, 3.7, and 3.2 (Paxinos and Watson, 1982)] were scanned on the experimental and control sides from each animal, and the results were expressed as profiles per section.

Western blotting

For western blots, we used the anti-rSyn(15–123) (Transduction Laboratories). For western blotting, individual pieces of SN were homogenized using a 1-ml syringe and 23-gauge needle in iced buffer (100 μl per piece) containing 10 m*M* Tris-HCl (pH 7.5), 2 m*M* EDTA, 0.5 m*M* EGTA, 20 μg/ml leupeptin hemisulfate, and 17 μg/ml phenylmethylsulfonyl fluoride. The homogenate was boiled for 5 min, supplemented with SDS to 1%, and kept on ice for 1 h. It was boiled again for 3 min and centrifuged for 10 min at 14,000 *g* at 4°C. Protein concentration of the supernatant was determined using a micro BCA kit (Pierce). The protein concentration for all samples was

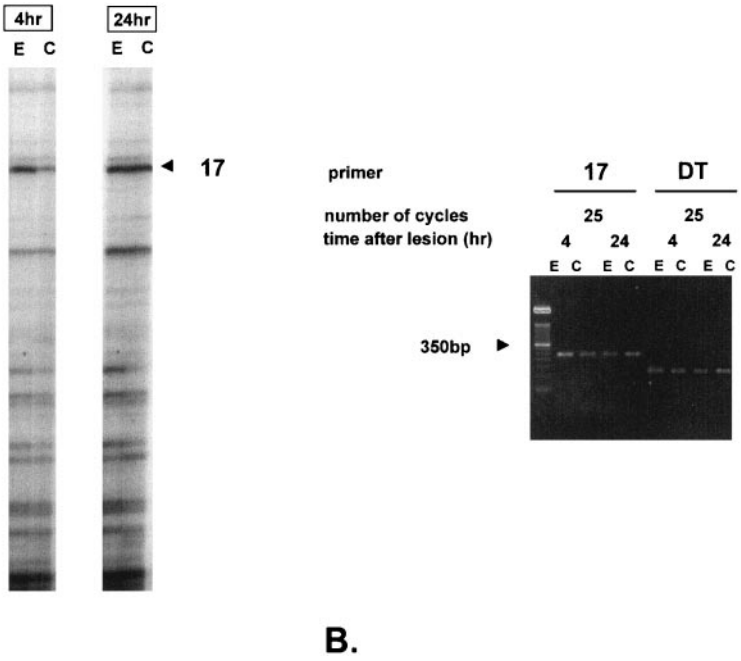

FIG. 1. Differential display of fragment 17 following induction of apoptotic cell death in SN by striatal target injury. **A:** A representative autoradiogram of mRNA differential display is shown for SN derived from single animals at 4 and 24 h following unilateral striatal lesion with QA on the experimental (E) side. C, control. Amplification products are more abundant on the E side at 4 h postlesion but are of equal abundance at 24 h. **B:** Comparative RT-PCR of fragment 17 using sequence-specific primers. There is an increased abundance of amplification products on the E side at 4 h postlesion. As a control, amplification for the dopamine transporter (DT) showed no side-to-side difference. Data are representative of multiple experiments.

diluted to 1 μg/μl with homogenization buffer. An equal volume of the sample buffer was added to the lysate, and samples were boiled for 1 min and electrophoresed in 15% SDS-polyacrylamide gel. After electrophoresis, proteins were transferred to polyvinylidene difluoride membrane (Amersham) using semidry electroblotting (E&K Scientific Products) and blocked overnight at 4°C in 0.1 *M* PBS (pH 7.5) with 0.1% Tween 20 containing 5% dry milk. Membranes were incubated with primary antibodies diluted with blocking solution for 1 h at room temperature and then washed three times for 15 min with blocking solution. Membranes were incubated with secondary antibodies conjugated to horseradish peroxidase (ECL kit; Amersham), diluted 1:2,000 in the same buffer, for 1 h at room temperature. Membranes were washed again in PBS with 0.1% Tween 20 buffer without milk. Bands were demonstrated by chemiluminescent detection (ECL system; Amersham) and exposure to MR x-ray film (Kodak).

Synuclein mRNA and protein expression in postnatal primary mesencephalic dopamine neuron culture

To examine the expression of synuclein mRNA and protein in defined dopamine neurons at a cellular level, we made use of a well-characterized primary culture model of postnatal mesencephalic dopamine neurons (Rayport et al., 1992; Sulzer et al., 1993). Cultures were established as previously described (Mena et al., 1997). Timed pregnant rats were obtained from Charles River Laboratories (Wilmington, MA, U.S.A.). The day of delivery was defined as PND 1. PND 2–3 animals were used for the preparation of glial monolayers. After 2 weeks, SN neurons were plated onto the glial monolayers. At 24 h before plating, glial growth medium was removed, and serum-free neuronal medium was added to each dish following a single rinse with serum-free neuronal medium. Serum-free neuronal medium was prepared as previously described (Burke et al., 1998). On the day of neuron plating, PND 2 rat pups were anesthetized by hypothermia, the brain was removed, and a 2–3-mm coronal section of the mesencephalon was taken. The coronal section was laid on a Sylgard block in ice-cold solution, and a horizontal cut was made to remove dorsal mesencephalon. SN neurons were then dissociated as described and plated at 80,000 cells per well. At 1 day in vitro, 5-fluorodeoxyuridine was added to each dish. Cultures were maintained at 36.7°C in 5% CO_2 until use. Cultures were maintained in serum-free medium at all times.

For single cell isolation and antisense RNA (aRNA) amplification, dopamine neurons were first immunostained for tyrosine hydroxylase (TH) as previously described (Przedborski et al., 1996). Single neuron isolation and amplification of aRNAs from the fixed, TH-stained SN neurons were performed according to established methods (Phillips and Eberwine, 1996) with few modifications. Following TH immunostaining, cells were rinsed in RNase-free water. In situ transcription (IST) was initiated directly in the cells by hybridizing T7-oligo$(dT)_{24}$ primer (2 ng/μl) in 100 μl of IST reaction buffer (50% formamide and 5 $\times$ SSC) to poly$(A)^+$ mRNA overnight at room temperature. After rinsing, cDNA synthesis was performed for 90 min at 37°C using 100 μl of cDNA synthesis buffer (1$\times$ IST reaction buffer, 7 m*M* dithiothreitol, 250 μ*M* deoxynucleotide triphosphate mix, 0.12 U/μl RNasin, and 0.5 U/μl avian myeloblastosis virus reverse transcriptase), followed by an overnight rinse in 0.5$\times$ SSC. Individual immunolabeled neurons were harvested by aspiration under a dissecting microscope using a micromanipulator and a recording microelectrode filled with HEPES (pH 7.4), 120 m*M* KCl, 1 m*M* $MgCl_2$, 250 μ*M* deoxynucleotide triphosphate mix, 100 ng/μl T7-oligo$(dT)_{24}$ primer, RNase-free water, and 0.5 U/μl avian myeloblastosis virus reverse transcriptase. cDNA synthesis continued for 90 min at 42°C, followed by phenol/chloroform extraction and ethanol precipitation. Double-stranded template cDNA was produced using second-strand buffer [100 μ*M* Tris-HCl (pH 7.4), 20 m*M* KCl, 10 m*M* $MgCl_2$, 5 m*M* dithiothreitol, and 250 m*M* deoxynucleotide triphosphate mix], 1 U/μl T4 DNA polymerase, and 1 U/μl Klenow fragment for 4 h at 15°C. Following degradation of single-stranded DNA and creation of blunt

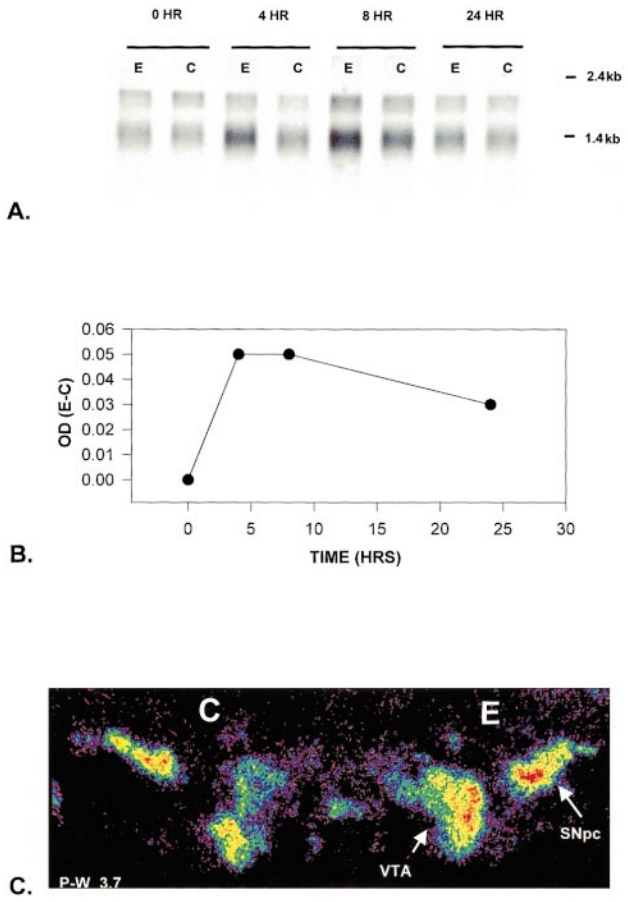

FIG. 2. Northern and in situ hybridization analysis of fragment 17 expression in midbrain following striatal target injury. **A:** Northern blot analysis of mRNA isolated from microdissected SN following striatal target lesion. Poly(A)$^+$ mRNA was loaded at 0.6 μg in each lane. Analysis shows an equal abundance of transcripts in SN on the experimental (E) and control (C) sides at $t = 0$ following striatal lesion. At 4, 8, and 24 h postlesion there is an increased abundance of transcripts on the E side. The difference in abundance is most marked at 4 and 8 h. Blots probed with a ^{33}P-labeled riboprobe generated from the fragment 17 sequence revealed two transcripts, one at 1.4 kb and a second at ~2.0 kb. The result shown was confirmed in two other independent experiments. **B:** Densitometric analysis of the 1.4-kb band in the northern blot shown in A. Data are expressed as the difference in optical density (OD) between the E and C sides. **C:** In situ hybridization for fragment 17 at 4 h postlesion. There is expression of mRNA in the SNpc and VTA on both the C and E sides, with an increased level of expression on the E side. In mesencephalic sections, expression was predominantly in these dopamine neuron-containing regions. At 24 h, there was no difference in the level of expression between the two sides (data not shown). Note that although synuclein is up-regulated on the E side, it is also abundantly expressed on the C side, in the absence of induced cell death or injury. Mesencephalic sections were cut at 14 μm and probed with the same riboprobe used in the northern analysis. P-W, Paxinos and Watson (1982), planes in the rat brain.

ends, the cDNAs were phenol/chloroform-extracted, ethanol-precipitated, and purified over QIA-quick PCR purification columns (Qiagen) by centrifugation. First-round aRNA synthesis was conducted for 4 h at 37°C with 2,000 U/μl T7 RNA polymerase (Epicenter), T7 buffer (Epicenter), 0.1 U/μl RNase inhibitor, and 2.3 m*M* deoxynucleotide triphosphate mix and then extracted and precipitated overnight. The aRNAs were subjected to first-round cDNA synthesis, using 50 ng of random hexanucleotide primers (Boehringer Mannheim) and 200 U/μl SuperScript II RNase H-reverse transcriptase (GIBCO). The reaction was incubated for 1 h at 37°C, followed by extraction and precipitation. Second-strand cDNA was synthesized, extracted, precipitated, and purified as described above. The second-round aRNA amplification was performed as above but with 3.3 m*M* ATP, GTP, and CTP, 0.2 m*M* UTP, and 1 mCi/100 μl [α-^{32}P]UTP (800 Ci/mmol). The radiolabeled aRNA probes were purified by centrifugation on Sephadex G-50, and specific activity was determined by liquid scintillation counting.

For reverse northern blot hybridization, amplified partial cDNAs for rat synucleins 1, 2, and 3, TH, vesicular monoamine transporter(VMAT)-2, glyceraldehyde 3-phosphate dehydrogenase (GAPDH), and hemoxygenase-2 (HO2), as well as plasmid vector pUC19, were immobilized on nylon membranes (Hybond N+; Amersham) at 30 μg per dot using 0.01 *M* EDTA and 0.4 *M* NaOH. Membranes were prehybridized in hybridization buffer (50% formamide, 7% SDS, 0.25 *M* NaCl, and 0.12 *M* Na_2HPO_4) for 30 min at 42°C. Heat-denatured aRNA probes (3.5×10^6 cpm) were diluted in hybridization buffer. Hybridization was conducted overnight at 42°C. Membranes were rinsed twice for 5 min with 0.2× SSC and exposed to phophorimaging cassettes for 24–72 h. Detection of radiolabeled aRNA was performed and analyzed with ImageQuant (Molecular Dynamics). cDNA probes were generated from total RNA derived from SN by RT-PCR using the following primers: synuclein 2, forward, 5′-ATGGGAGAGTGCACAAACCA-3′; reverse, 5′-CTCCGTAAGTACGGTAATGT-3′; synuclein 3, forward, 5′-AGGTAGTGACACTGTGACTA-3′; reverse, 5′-TCCCTGTTTGTTTCTGAGAG-3′; TH, forward, 5′-ATTGGACTTGCATCTCTGGG-3′; reverse, 5′-CAGGGTGTACGGGTCAAACT-3′; VMAT2, forward, 5′-CGGCGAGCATCTCTTATCTC-3′; reverse, 5′-GCAGAGGGACCGATAGCATA-3′; GAPDH, forward, 5′-AAGGTCATCCCAGAGCTGAA-3′; reverse, 5′-CCCTGTTGCTGTAGCCGTAT-3′; and HO2, forward, 5′-CTCAGCGGGCACTAAAACTC-3′; reverse, 5′-TCCCAGGGTACCTTTGTCTG-3′.

For double labeling of synuclein and TH, the cultures were fixed with 4% paraformaldehyde in phosphate buffer. The cultures were treated with Tris-buffered saline containing 2% normal goat serum and 2% normal horse serum (Vector Laboratories) and then incubated with primary antibodies against synuclein [anti-rSYN(15–123); Transduction Laboratories] at 1:200 and against TH (anti-rat TH; Calbiochem) at 1:1,000 at 4°C for 48 h. After washes, the cultures were incubated with Texas Red horse anti-mouse antibody (Vector) at 1:75 (to demonstrate the anti-synuclein mouse monoclonal) and with fluorescein goat anti-rabbit antibody (Vector) at 1:75 (to demonstrate the anti-TH rabbit polyclonal). Dishes were then viewed with a Zeiss Axiovert inverted microscope with xenon arc lamp illumination and appropriate filters. An identical protocol was used to demonstrate double labeling for synuclein and TH in tissue sections.

RESULTS

mRNA differential display and RT-PCR of fragment 17

Application of mRNA differential display identified 147 differentially displayed bands, from which 191 dis-

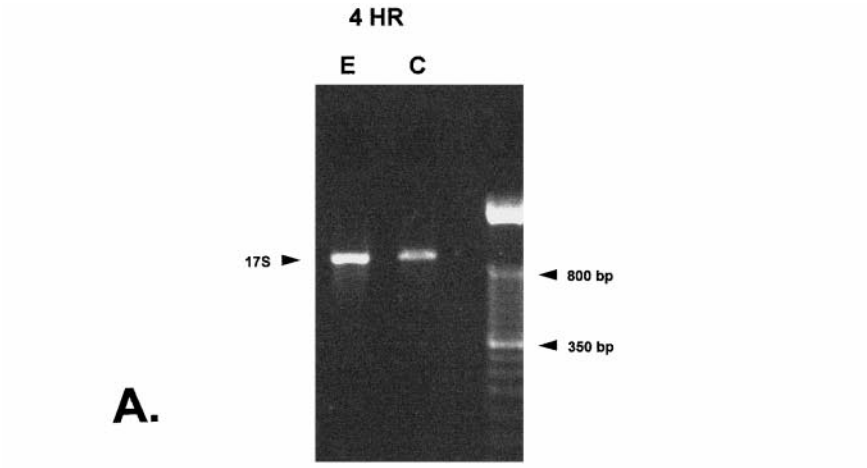


```
  1                                                   M   D   V   F   M   K   G       7
  1  GTG TGG AGC AAA GAT ACA TCT TTA GCC ATG GAT GTG TTC ATG AAA GGA                  48

  8  L   S   K   A   K   E   G   V   V   A   A   A   E   K   T   K                  23
 49  CTT TCA AAG GCC AAG GAG GGA GTT GTG GCT GCT GCT GAG AAA ACC AAG                  96

 24  Q   G   V   A   E   A   A   G   K   T   K   E   G   V   L   Y                  39
 97  CAG GGT GTG GCA GAG GCA GCT GGG AAG ACA AAA GAG GGC GTC CTC TAT                  144

 40  V   G   S   K   T   K   E   G   V   V   H   G   V   T   T   V                  55
145  GTA GGT TCC AAA ACT AAG GAG GGA GTC GTT CAT GGA GTG ACA ACA GTG                  192

 56  A   E   K   T   K   E   Q   V   T   N   V   G   G   A   V   V                  71
193  GCT GAG AAG ACC AAA GAG CAA GTG ACA AAT GTT GGA GGG GCA GTG GTG                  240

 72  T   G   V   T   A   V   A   Q   K   T   V   E   G   A   G   N                  87
241  ACT GGT GTG ACA GCA GTC GCT CAG AAG ACA GTG GAG GGA GCT GGG AAC                  288

 88  I   A   A   A   T   G   F   V   K   K   D   Q   M   G   K   G                  103
289  ATT GCT GCT GCC ACT GGT TTT GTC AAG AAG GAC CAG ATG GGC AAG GGT                  336

104  E   E   G   Y   P   Q   E   G   I   L   E   D   M   P   V   D                  119
337  GAA GAA GGG TAC CCA CAA GAG GGA ATC CTG GAA GAC ATG CCT GTG GAC                  384

120  P   S   S   E   A   Y   E   M   P   S   E   E   G   Y   Q   D                  135
385  CCT AGC AGT GAG GCT TAT GAA ATG CCT TCA GAG GAA GGC TAC CAA GAC                  432

136  Y   E   P   E   A   *                                                          141
433  TAT GAG CCT GAA GCC TAA GAA TGT CGT TGC ACC TAC TGT CCT AAG ATC                  480

481  TGC CCA GGT GTT CTT CCA TGG CGT ACA AGT GCT CAG TTC CAA CGT GCC                  528

529  CAG TCA TGA CCT TTT CTC AAA GCT GTA CAG TGT ATT TCA AAG TCT TCC                  576

577  ATC AGC AGT GAT CGG AGT CCT GTA CCT GCC CCT CAG CAT CCC GGT GCT                  624

625  CCC CTC TCA CTA CAG TGA ATA CAT GGT AGC AGG CTC TTG TGT GCT GTG                  672

673  GAT ATT GTT GTG GCT TCA AAC CTA AAA TGT TAG AAG AAA CTT AAA ACA                  720

721  CCT AAG TGA CTA CCA CTT ATT TCC AAC TCT TCA CCG TTT TTG GTT GCT                  768

769  GTT CTC AAG AAG TTG TGA TTT GCT ATA AGA CTT TTA GAT GTC CTT AAT                  816

817  GAT TCT TTC TGT CTA AGA AGA ATG ATG TGC TGT GAA ATT TGT TAA TAT                  864

865  ATA TTT TAA AAT ATG TGA GCA TGA GAC TAC GCA CCT ATA AAT ATT AAT                  912

913  TTA TGA ATT TTA CAG TTT TGT GAC GTG TTT TAT TAA CTT GTG TTT GTA                  960

961  TAT AAA TGG TGG AAA TTA AAA TAA AAT AAA AAC ATT ATC TCA TTG CAA                  1008

1009 AAA AAA AAA A                                                                 1018
```

B.

FIG. 3. The fragment 17 sequence derives from the 3′ end of synuclein 1. **A:** Comparative RT-PCR for synuclein 1 following induction of apoptosis in SN. The fragment 17 reverse primer, in conjunction with a forward primer based on a shared sequence within the synucleins (Maroteaux and Scheller, 1991), succeeded in the amplification of a 900-bp product (17S). Comparative RT-PCR confirms a greater abundance of product at 4 h postlesion on the experimental (E) side. C, control. **B:** The sequence of rat α-synuclein, the synuclein 1 splice variant. The sequence from nucleotides 1 to 718 represents the coding and 3′ untranslated region of the original sequence for rat α-synuclein reported by Maroteaux et al. (1988) (nucleotides 1,465–2,215). Nucleotides 664–1,018, shown in italics, represent fragment 17. The two sequences overlap from nucleotides 664 to 718, shown in bold. Although the fragment 17 sequence overlaps with the partial sequence reported by Maroteaux et al. (1988) for 54 bases, a BLAST search with the fragment 17 sequence did not reveal this homology because the sequence reported previously is not represented in GenBank. The sequence in GenBank for the synuclein 1 splice variant derives from Maroteaux and Scheller (1991) (accession no. S73007). However, in Fig. 1 of that publication (from which the GenBank entry was derived) the sequence of synuclein 1 was reported only through nucleotide 2,124 and therefore did not overlap with the fragment 17 sequence. In addition, the final 100 bases of the synuclein 1 and 2 splice variants were transposed. The forward and reverse primers used to amplify the fragment 17 sequence for RT-PCR (Fig. 1B) are underlined with solid lines; the 5′-end forward primer used in conjunction with 17R to produce the 900-bp product shown in A is underlined with a dotted line.

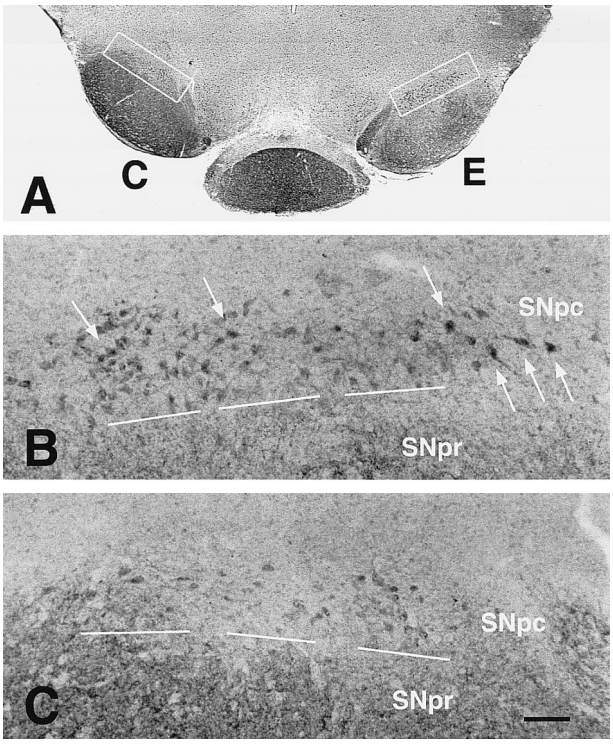

FIG. 4. Immunohistochemistry for rat synuclein at 24 h postlesion. **A:** Sections were immunostained with a rabbit anti-NACP(131–140) polyclonal antibody at 1:125 (Iwai et al., 1995*a*) (kindly provided by the laboratory of Dr. T. Saitoh) for 48 h at 4°C. At low magnification, immunostaining of mesencephalon shows a reduction in stained neuropil in the SNpr on the experimental (E) side at 24 h, which is likely to be due to the loss of the striatonigral afferent projection following QA lesion. In SNpc, there is an increased abundance of synuclein-positive neurons in comparison with the control (C) side. A similar pattern of staining was observed with the mouse monoclonal antibody to rat synuclein(15–123) [anti-rSyn(15–123)] (Transduction Laboratories). The SNpc on the E side (enclosed in a white rectangle) is shown at higher magnification in **B;** the C side is shown in **C.** B: Synuclein staining on the E side at 24 h. Darkly staining neurons in the SNpc are indicated by arrows. In the SNpr, only punctate fiber and terminal staining is observed. C: Synuclein staining on the C side. Very few, faintly stained neuronal profiles are observed in SNpc. Dense punctate fiber and terminal staining is observed in SNpr. Bar = 100 μm.

tinct sequences were identified. BLAST (Altschul et al., 1990) analysis of sequences in GenBank revealed 104 homologies to known sequences; of these, 23 were deemed of particular interest based on known relationships to neurologic disease, the cell cycle, or apoptosis. One of the amplified fragments (fragment 17) was differentially displayed in three of four animals at 4 h posttarget lesion but not at 24 h (Fig. 1A). This 354-bp fragment was identified by BLAST to bear significant homology to NACP (Ueda et al., 1993). To confirm the differential display of this fragment in SN following target lesion, comparative RT-PCR was repeated using specific primers for fragment 17. This analysis confirmed an increased abundance of the amplified fragment at 4 h postlesion (Fig. 1B).

Northern analysis and in situ hybridization

The relative abundance of mRNA transcripts containing the sequence of fragment 17 was examined. As demonstrated in Fig. 2A, two transcripts were demonstrated: a major one at 1.4 kb and a second, minor one at ~2.0 kb. The abundance of both the major and minor transcripts was equal in SN tissues at $t = 0$ relative to the striatal lesion. Increased expression of the 1.4-kb transcript was observed at 4, 8, and 24 h on the side of the target injury, with the most pronounced difference at 4 and 8 h. Increased expression of the 2.0-kb transcript was definite only at 4 and 8 h. Given that differential display, RT-PCR, and northern analysis of poly(A) mRNA revealed an increased relative abundance of transcripts containing the fragment 17 sequence, we next determined whether this was due strictly to an increase in the experimental SN or, alternatively, whether this increase was accompanied by increases, at a lower level, in the contralateral control SN. For this analysis, three northern blots were performed at 4 h postlesion, each containing two vehicle-injected controls (total n = 6) and from two to five QA-injected animals (n = 9). Each blot was probed with the fragment 17 sequence, stripped, and reprobed for GAPDH. There was no difference between the control side of QA-injected animals and either side of vehicle-injected animals, when the data were expressed in absolute terms as optical density of the fragment 17 band or when normalized for GAPDH optical density. This analysis also reconfirmed an increased expression of fragment 17 following striatal target injury on the ipsilateral side ($p < 0.03$ by paired t test).

To confirm further differential expression at the mRNA level and to examine the regional localization, in situ hybridization was performed. At 4 h postlesion, there was a clear increase in expression of the fragment 17 sequence within the SNpc and the ventral tegmental area (VTA) (Fig. 2C). Increased expression in SNpc was confirmed by image analysis, which revealed a greater OD on the experimental side (0.23 ± 0.02) in compari-

TABLE 1. *Synuclein and NAC immunoreactivity and apoptotic morphology as analyzed by colabeling*

Antibody	n	Syn or NAC(+) Apo (−)	Syn or NAC(+) Apo (+)	Syn or NAC(−), Apo (+)
Synuclein(15–123)	2	232	0	212
NAC(61–69)(I)	4	274	1	368

For analysis of the relationship between synuclein staining and apoptotic morphology, two brains were processed at 24 h after striatal lesion, stained with the anti-rSyn(15–123) (Transduction Laboratories) antibody, and thionin-counterstained. Sections from planes 4.2–3.2 (Paxinos and Watson, 1982) were scanned at 600× for synuclein-positive and apoptosis-positive profiles up to a count of at least 100 for each profile type in each brain. There was not a single occurrence of colabeling. For the analysis of the relationship between NAC staining and apoptotic morphology, four brains were processed at 24 h after striatal lesion, stained with the Iwai anti-NAC(61–69)(I) antibody, and thionin-counterstained. Sections were scanned at 600×. There was only one instance of colabeling.

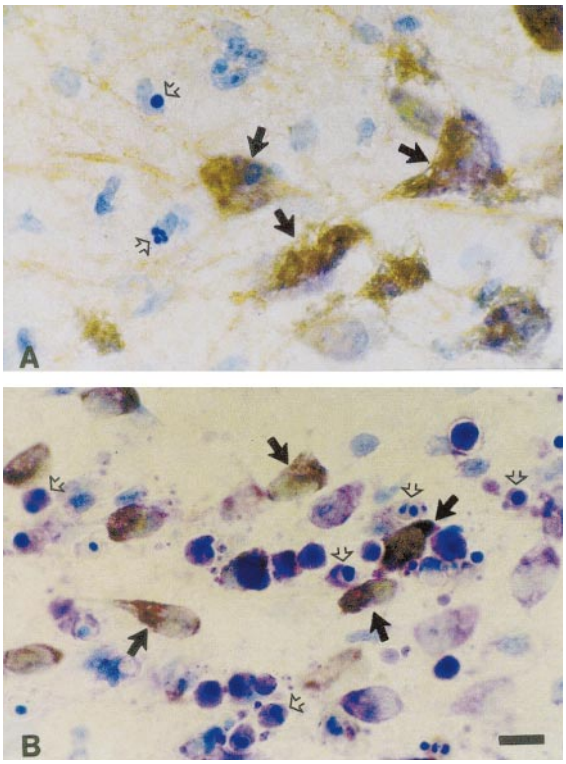

FIG. 5. Immunostaining for synuclein and NAC with thionin counterstain to identify apoptotic chromatin clumps. **A:** The SN is immunostained for synuclein with the anti-rSyn(15–123) antibody (Transduction Laboratories) at 24 h poststriatal lesion. Immunoperoxidase-stained neurons are indicated by solid black arrows. None of these neurons reveals apoptotic chromatin clumps within the nucleus. Conversely, two apoptotic profiles, indicated by rounded intensely basophilic chromatin (open arrows), are synuclein-negative. **B:** The mamillary body is immunostained for NAC with the anti-NAC(61–69)(l) antibody. Four NAC-positive neuronal profiles (solid arrows) show no apoptotic chromatin clumps. Conversely, numerous apoptotic profiles (five within the plane of focus are marked with open arrows) are NAC-negative. Bar = 10 μm.

son with control (0.17 ± 0.01; $p = 0.03$). The increased expression in VTA was not unexpected, because our striatal lesion extends into the nucleus accumbens, a known VTA target. As in the northern analysis, expression was also observed on the contralateral control side. On both sides, in the midbrain, label was primarily localized to SNpc and VTA, both regions populated by dopamine neurons. Low levels of expression were also observed in SN pars reticulata (SNpr), but there was no increase on the side of the striatal lesion.

Identification of fragment 17 as the 3′ end of synuclein 1

Although fragment 17 was highly homologous to the 3′ untranslated region of the human NACP gene, we found no corresponding rat sequence in GenBank. We considered the possibilities that fragment 17 represented either a previously unsequenced 3′ end of one of the known rat synucleins or a sequence from a novel member of the synuclein family. To distinguish between these possibilities, we performed PCR on cDNA derived from SN using a 5′-end forward primer representing a common sequence within the 5′ untranslated region of the rat synucleins (Maroteaux and Scheller, 1991) and our original fragment 17 3′-end reverse primer. This strategy resulted in the successful amplification of a single 900-bp fragment (Fig. 3A). Comparative RT-PCR confirmed an increased relative abundance of this larger fragment in SN on the side of induced death at 4 h following target injury. Cloning and sequencing of this fragment revealed that its sequence is identical to that of synuclein 1 from bases 1 to 718 (Fig. 3B) (Maroteaux et al., 1988). Thus, fragment 17 corresponds to a previously unsequenced portion of the 3′ untranslated end of rat synuclein 1 (sequence data submitted to GenBank under accession no. AF007758).

Immunohistochemistry and western blotting for synuclein

To assess the functional significance of increased mRNA expression for synuclein 1, we examined protein expression by immunohistochemistry with the anti-NACP(131–140) antibody (Iwai et al., 1995*a*,*b*). Examination of the SN at 4 h postlesion revealed dark staining of fibers and punctate structures within the SNpr on both sides, suggestive of neuropil staining as previously described for other brain regions by others (Maroteaux and Scheller, 1991; Iwai et al., 1995*a*,*b*). Neurons within the SNpc were faintly and equally stained on both sides. At 24 h postlesion, two changes were observed (Fig. 4A): There was decreased fiber and punctate staining in the SNpr, and there was an increased number of synuclein-positive neuronal profiles within the SNpc (experimental, 19.0 ± 4.2 profiles per section; control, 6.8 ± 1.4 profiles per section ($p < 0.01$). Our interpretation of the diminished fiber staining in the SNpr is that a major source of afferents is the striatum; following striatal lesion, there is a reduction in number of these synuclein-positive fibers. The appearance of the synuclein-positive cells within the SNpc was uniformly neuronal (Fig. 4B). Representative sections were Nissl-counterstained to attempt to identify characteristic apoptotic chromatin clumps; we have previously used this technique to identify apoptotic profiles within peroxidase-stained neurons (Macaya et al., 1994) and specifically within apoptotic neurons expressing the death effector caspase-3 (Marti et al., 1997; Jeon et al., 1999). However, apoptotic chromatin clumps were not identified within synuclein-positive neurons, and, conversely, synuclein peroxidase staining was not observed around chromatin clumps. The pattern of immunostaining observed with anti-NACP(131–140) was also observed with anti-rSyn(15–123). Because cell body staining was more distinct with this antibody, we performed a quantitative analysis of the relationship between synuclein immunoreactivity and apoptotic profiles, defined by thionin staining of apoptotic chromatin clumps (Table 1). There was no instance of double labeling (Fig. 5A). We performed a similar analysis using staining with anti-NAC(61–69). Only one

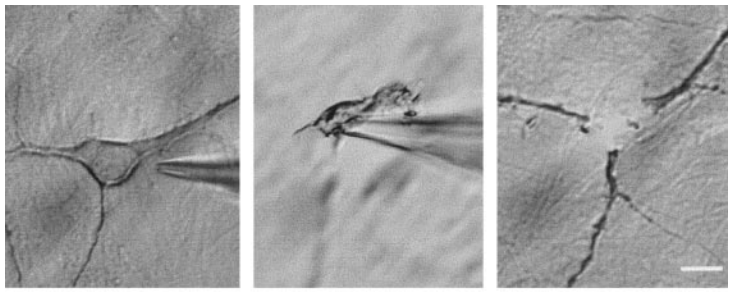

A

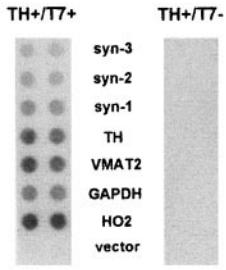

B

FIG. 6. Demonstration of synuclein (syn) mRNA in a TH-immunolabeled neuron in mesencephalic postnatal primary culture. **A:** Isolation of a single TH-positive mesencephalic neuron from the culture dish. **Left panel:** Outline of the approaching micropipette (the dark tapered structure on the right) adjacent to a fixed, TH-positive neuron. **Middle panel:** The same cell has been impaled and removed from the monolayer by the micropipette. **Right panel:** Cell remnants, such as TH-positive processes. Bar = 5 μm. **B:** Reverse northern analysis of aRNA obtained from the neuron shown in A. Heat-denatured, radiolabeled aRNA probes, prepared as described in Materials and Methods, were hybridized overnight to membrane-bound cDNAs. Positive hybridization was detected for syn 1 and at a lower level for the splice variants syn 2 and 3. Positive hybridization was also detected for TH and VMAT2 and both HO2 and GAPDH. Control hybridizations with a sequence of the bacterial vector (pUC19) and control reactions performed in the absence of T7 RNA polymerase were negative. Each reaction was performed in duplicate, as shown. Similar results were obtained in two other TH-positive neurons.

NAC-positive profile contained apoptotic chromatin clumps (Table 1). The discordance between apoptotic morphology and NAC expression was particularly striking in the mamillary body (Fig. 5B), where death is also observed in this model.

We also identified synuclein-positive fibers within the medial forebrain bundle and the striatum, both of which contain fibers of the nigrostriatal dopaminergic projection. There was no apparent difference in the amount of fiber staining in these structures between the two sides.

Synuclein expression was also examined by western blotting with the anti-rSyn(15–123) antibody in SN at 24 h after target injury. A single band was observed at the expected molecular mass (19 kDa). There was no apparent change in the abundance of synuclein protein on the side of the lesion (data not shown). It is probable that the opposing changes in protein expression in SNpc and SNpr, detected by immunostaining, obscured any change observable at the regional level by western analysis. In addition, western analysis examined only the heat-soluble fraction, not total cell lysate.

Expression of synuclein 1 mRNA and protein in dopamine neurons

To determine at a cellular level whether synuclein 1 mRNA and protein are expressed in mesencephalic dopamine neurons, we made use of a primary postnatal culture model. In culture these neurons resemble their in vivo counterparts in soma morphology, axodendritic differentiation, synaptic arrangements with nondopaminergic cells, and synaptic specializations (Rayport et al., 1992; Pothos et al., 1998). To identify synuclein mRNA at the cellular level, we made use of the single-cell mRNA amplification technique (Phillips and Eberwine, 1996). The results for a single sampled TH-positive neuron are shown in Fig. 6. Reverse northern analysis of the mRNA sampled from this single neuron demonstrates coexpression of mRNAs associated with the dopaminergic phenotype (TH and VMAT2) with mRNA for synuclein 1. Identical results were obtained for two other TH-positive neurons. To confirm that synuclein 1 mRNA was functional and produced a translation product, we performed immunofluorescence double labeling for synuclein and TH. Figure 7 demonstrates that synuclein protein was identifiable in both cytoplasm and nucleus in these neurons in culture. To confirm that these results were relevant to synuclein expression in vivo, we performed double labeling on SN tissue sections from normal PND 7 rats. These studies also demonstrated coexpression of synuclein and TH in dopamine neurons of the SN (Fig. 7).

Expression of synuclein 1 mRNA during normal postnatal development of the SN

To examine further the relationship between synuclein 1 mRNA expression and apoptotic death in SN, we analyzed natural developmental cell death in the SN (Janec and Burke, 1993; Oo and Burke, 1997). Cell death in this setting is likely to share the molecular features of death induced by target injury because the latter is pos-

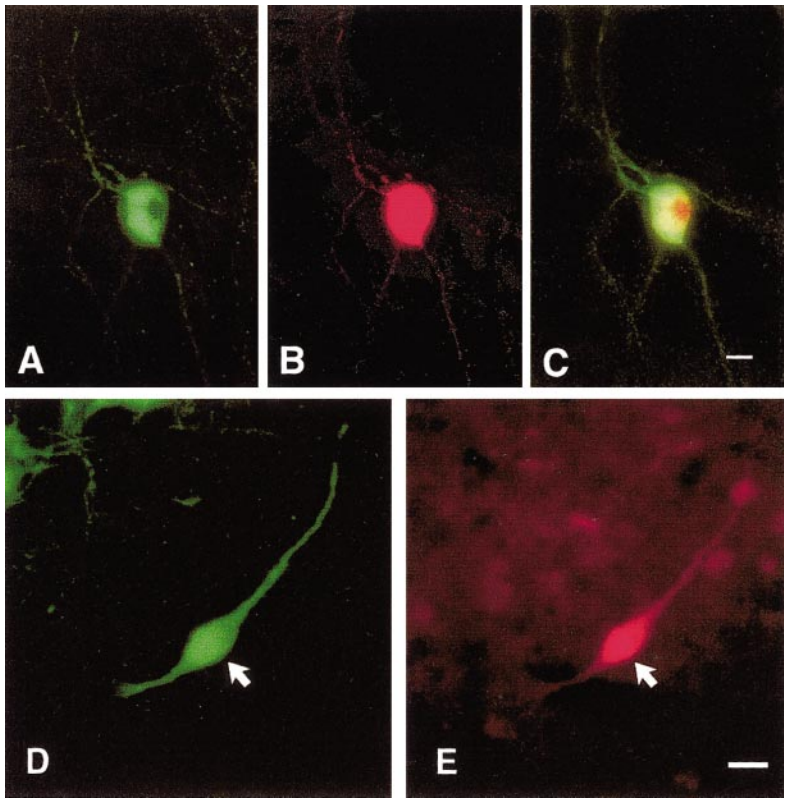

FIG. 7. Double immunofluorescence staining of TH and synuclein in postnatal rat mesencephalic culture and in SN tissue sections. **A:** TH immunoreactivity in a mesencephalic dopamine neuron in primary culture. **B:** Synuclein immunoreactivity in the neuron shown in A. There is staining not only of the cell cytoplasm and neural processes, but also the nucleus. **C:** Merged image of A and B. Cellular regions of colabeling, such as the cytoplasm, are now indicated by yellow. Note that the nucleus retains a red color, indicating that nuclear staining is positive only for synuclein. Bar = 10 μm. **D:** TH immunoreactivity in a neuron in the SNpc. **E:** The neuron shown in D demonstrates positive immunofluorescent staining for synuclein. The red background in this micrograph represents numerous synuclein-positive fibers out of the plane of focus. Bar = 20 μm.

tulated to be an augmented natural cell death event (Clarke, 1985). We have previously shown that natural cell death in the SNpc has a distinct biphasic temporal profile, with peaks at PND 2 and PND 14. During development, the difference in prevalence of apoptotic profiles between the peak at PND 2 and the lowest levels at PNDs 20–28 is approximately an order of magnitude, which is equal to the level of induction observed in the target injury model (Macaya et al., 1994). We observed that synuclein 1 mRNA is up-regulated from PND 2 to 4 (Fig. 8A) and then remains at this level through PND 30. In adult animals, expression is lower (Fig. 8A, C, and E). In a separate analysis, synuclein expression was examined on a daily basis from PND 2 to 16 (Fig. 8D). We observed no up-regulation during periods of maximal natural cell death on PNDs 2 and 14 (Fig. 8D and F). Thus, whereas synuclein 1 mRNA is up-regulated postnatally during a period of marked structural growth and plastic change for dopamine neurons, its expression is not correlated with cell death.

Transglutaminase expression

To evaluate further the functional significance of increased synuclein 1 expression in the target injury model, we considered the possibility that it may serve as a substrate for protein cross-linking by tissue transglutaminase (Jensen et al., 1995). Tissue transglutaminase has previously been shown to be up-regulated during apoptosis and has been immunohistochemically identified within apoptotic profiles (Fesus et al., 1991). Although we observed positive staining within the immature cerebellum, as previously described by others (Perry and Haynes, 1993), we did not observe positive staining in the SNpc, either in intact neurons or in apoptotic profiles (data not shown).

DISCUSSION

These results show that by 4 h following axon-sparing injury to the target striatum, there is an induction of mRNA for synuclein 1 within the SNpc. This increased expression is identified not only by RT-PCR, but also by northern analysis and in situ hybridization with a probe based on a previously unidentified 3′ end sequence of rat synuclein 1. Northern analysis detected two transcripts in SN tissue, one at 1.4 kb and a second at 2.0 kb. Similarly, Maroteaux et al. (1988) demonstrated two transcripts, one at 1.4 and another at 2.1 kb in *Torpedo.* However, in rat brain they reported only one band at 1.7 kb (Maroteaux and Scheller, 1991); they may have not observed two transcripts because they examined total brain and used total RNA for their analysis. The increase in expression of synuclein 1 mRNA in our model is further confirmed by RT-PCR based on a 900-bp sequence of rat synuclein 1. Maroteaux and Scheller (1991) have shown previously that three splice variants exist for rat synuclein; however, the fragment 17 sequence, which represents the 3′ end of rat synuclein 1, is not shared by synuclein 2 or 3, so our northern and in situ analyses are specific for synuclein 1.

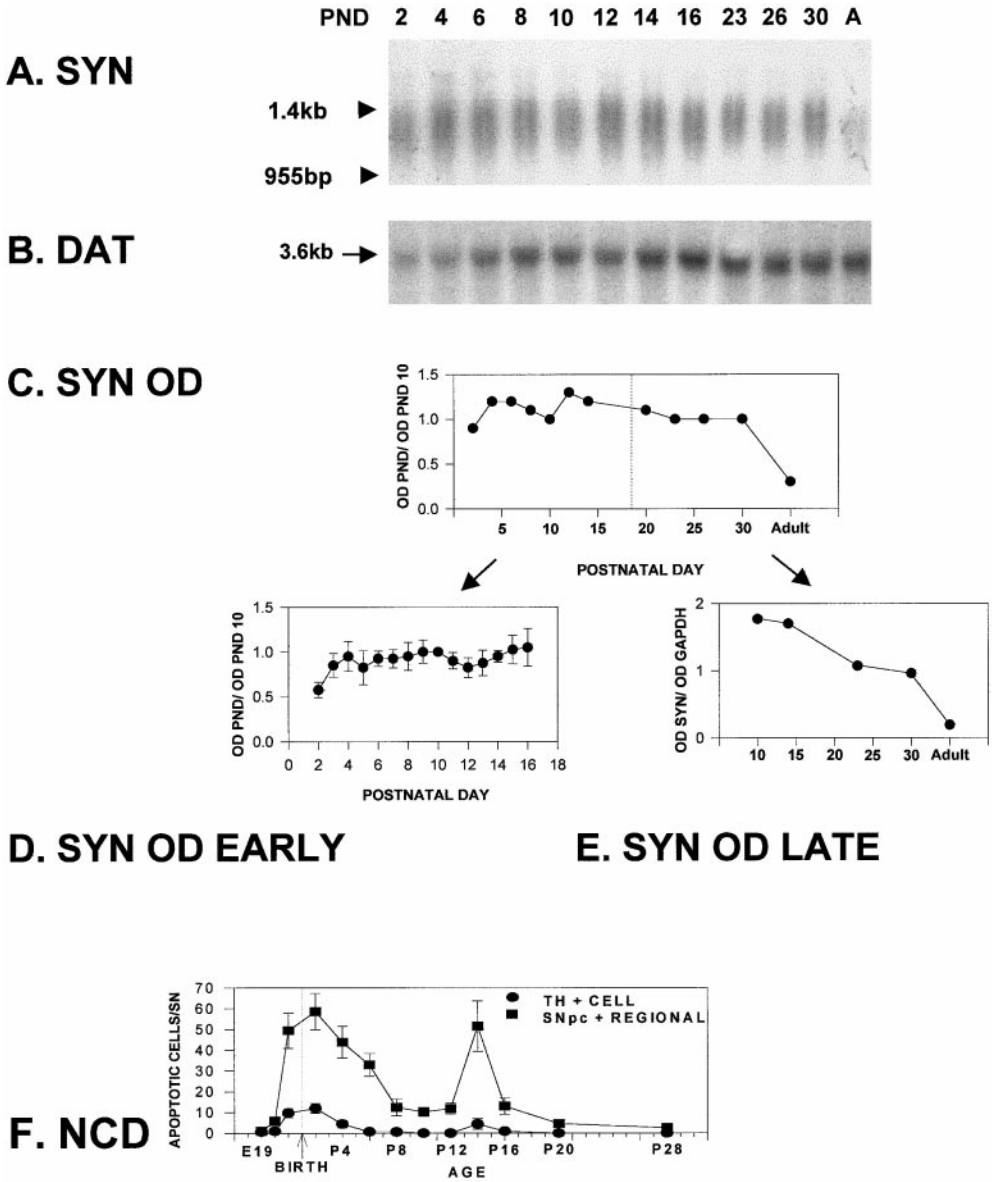

FIG. 8. Expression of synuclein 1 (SYN) mRNA in SN during normal development. **A:** A representative northern analysis of SYN mRNA expression from PND 2 to adulthood (A). Ten micrograms of total RNA, obtained from the SN of a single animal, was loaded per lane, and the blot was probed with a riboprobe generated from the cloned fragment 17. The density of the band increases from PND 2 to 4, remains elevated through PND 30, and then decreases in adulthood. Equal loading of the gel was confirmed by examination under UV following ethidium bromide staining. **B:** Northern analysis of the expression of the dopamine transporter (DAT) during normal development. The blot shown in A was stripped and reprobed with a riboprobe for the DAT. DAT expression gradually increases during early postnatal development and, in contrast to SYN, remains at a high level of expression in adulthood. **C:** The optical densities (ODs) of the bands shown in A are here plotted as a ratio normalized to the density of the band at PND 10. **D:** ODs for four northern analyses performed on animals from PND 2 to 16. Within each northern blot all PNDs from 2 to 16 were represented by single animals. For each analysis, all densities were expressed as a ratio by normalizing to the PND 10 density. Data are mean ± SE (bars) values of the four ratios. This analysis confirms up-regulation of SYN mRNA from PND 2 to 4. There is no significant difference in the density ratios from PND 4 to 16 ($p = 0.25$, not significant, ANOVA). Therefore, there is no up-regulation of SYN at the times of maximal natural cell death at PNDs 2 and 14. **E:** In separate experiments, northern analyses were performed on SN tissues obtained at PNDs 10, 14, 23, and 30 and from adults. Each blot was probed with the fragment 17 sequence, stripped, and probed again for GAPDH. The ODs for SYN were normalized for those of GAPDH. A representative experiment is shown. These studies confirmed down-regulation following the postnatal period. **F:** The time course of natural cell death (NCD) among dopamine neurons of the SNpc (reproduced with permission from Oo and Burke, 1997).

That the increased expression of synuclein 1 mRNA may be functionally significant is suggested by our finding that there is an increase in the number of synuclein-positive neuronal profiles in SNpc at 24 h after target injury, as demonstrated by anti-NACP(131–140) immunostaining. This assessment by immunohistochemistry

does not permit quantification of protein, but it is required to demonstrate the regional differences in expression between SNpc and SNpr. At 24 h, there is a decrease in the number of synuclein-positive fibers in SNpr. Because the striatum provides major afferent input to SNpr and the striatal QA lesion results in degeneration of striatonigral terminals by 24 h, it is likely that loss of SNpr synuclein staining is due to loss of this projection. This interpretation is compatible with the observation that synuclein 1 mRNA is expressed in intrinsic striatal neurons (Maroteaux and Scheller, 1991).

Our results demonstrate a close temporal and regional correspondence between induction of apoptotic neuron death in the SN and both mRNA and protein expression of synuclein in the target injury model. However, our data do not support a conclusion that synuclein is playing a direct role in cell death. First, in the target injury model, at a cellular level, there was virtually a complete dissociation between synuclein (or NAC-related protein) expression and apoptotic morphology. It might be argued that synuclein expression is early and transient in the death process and no longer demonstrable by immunostaining when the cell reaches a later stage of apoptotic morphology. However, in this model, we have found it possible to demonstrate several cell proteins in apoptotic profiles, including TH (Macaya et al., 1994), which is expressed before onset of the death process, and c-Jun (Oo et al., 1999), which is expressed early in the course of cell death (Estus et al., 1994) and is a short-lived protein (Morgan and Curran, 1995). We have also demonstrated a close association between apoptotic morphology and a known mediator of apoptosis, activated caspase-3 (Jeon et al., 1999). Thus, it seems unlikely that a protein involved in cell death would be so rarely observed in apoptotic profiles. Second, we have observed a discordance between synuclein mRNA expression and the occurrence of cell death at the regional level during normal development. Third, in the target injury model, there is expression of synuclein mRNA and protein in the contralateral, unlesioned SNpc. Although there are low levels of natural cell death on the control side (Macaya et al., 1994), the number of apoptotic profiles is only ~10% of that on the side of target injury. However, the number of synuclein-positive profiles on the control side was 35% of the number on the experimental side. Thus, there is a disparity between levels of induced cell death in SNpc in the model and the numbers of protein-positive profiles. Nevertheless, we recognize that a direct role for synuclein in mediating cell death cannot be definitively or generally excluded based on these studies alone; further analysis in other paradigms will be required.

If synuclein and related proteins are not expressed in dying cells and are instead expressed in cells that will remain viable, there are at least two classes of cellular response in which they may play a role. In models of neural injury, neurons that remain viable may show injury responses, thought to play a role in maintaining viability, and plasticity responses, which mediate sprouting or other structural reorganization. A role for synuclein in an injury response may be compatible with our observations in the target injury model, but such a role seems unlikely. In another model of apoptotic death in dopamine neurons of the SNpc, induced by intrastriatal injection of 6-hydroxydopamine (Marti et al., 1997), dopamine terminals are directly injured by striatal injection of toxin, and yet no up-regulation of synuclein mRNA or protein is observed (Kholodilov et al., 1999). Furthermore, the abundant expression of synuclein in the normal SN indicates that injury is not required for its expression. Observations in the target injury model are compatible with a possible role for synuclein in a plasticity response. In that model, there is a loss of SNpc dopamine neurons, and those neurons that survive are likely to undergo compensatory structural change. Our observations in normal development are also consistent with a role in neural plasticity. Synuclein mRNA is up-regulated in SN during the postnatal period, when nigrostriatal neurons are developing target contact, sprouting, and forming synapses (Coyle, 1977). Similar to our results in SN, other investigators have shown by in situ hybridization that synuclein mRNA expression is up-regulated in the postnatal period in cortex and hippocampus (Petersen et al., 1999). The possibility that synuclein may play a role in neural plasticity in the target injury model is compatible with the observation that the avian homologue, synelfin, is likely to play such a role (George et al., 1995). A role in neural plasticity is also suggested by the observation of Maroteaux et al. (1988) that the KTKEGV repeat sequence in synuclein bears homology to the Rho family of proteins, which have been postulated to play a role in neuritogenesis (Mackay et al., 1995). Such a role is also compatible with the recent observation that synuclein inhibits phospholipase D_2 (Jenco et al., 1998). Phospholipase D_2 has been proposed to play a role in cytoskeletal organization (Colley et al., 1997). However, it appears unlikely that synuclein plays a direct role in a sprouting response. GAP43 expression is frequently induced in sprouting responses but was not increased in the target injury model at a time when synuclein expression was (authors' unpublished data). In hippocampal neuron culture, synuclein is expressed late, days after expression of synapsin I, suggesting that synuclein does not play a direct role in the formation of synaptic terminals (Withers et al., 1997). Thus, the precise cellular role of synuclein in neuronal plasticity as we and others (George et al., 1995) have postulated remains to be defined.

Our immunostaining results demonstrate synuclein protein expression exclusively in neurons, both in tissue sections and in culture, and some of these neurons can be demonstrated to be dopaminergic by double labeling for TH, but we cannot generalize from these results that synuclein is never expressed in other brain cells. It is known that abnormal synuclein-positive aggregates form in oligodendroglia in some degenerative neurologic diseases, such as the multiple system atrophies (Tu et al., 1998). The source of α-synuclein protein in oligodendroglia remains to be determined. In dopamine neurons,

our single-cell data indicate that synuclein 1 mRNA is present within the cell.

The neurobiology of synuclein has taken on great importance in relation to degenerative disease. The human form was originally identified in senile plaques of Alzheimer's disease (Ueda et al., 1993), and two different mutations of the synuclein gene have been reported to cause familial Parkinson's disease (Polymeropoulos et al., 1997; Kruger et al., 1998). In addition, synuclein has been identified as a major component of Lewy bodies (Spillantini et al., 1997), a pathologic hallmark of Parkinson's disease and other neurodegenerative disorders. The role of synuclein in these diseases is unknown. Its role may relate to properties of the protein that may be toxic to the cell, independent of its normal function. Both the internal NAC sequence (Han et al., 1995; Iwai et al., 1995*a*,*b*) and full-length synuclein (Hashimoto et al., 1998) are capable of spontaneously forming amyloidogenic protein aggregates, which may be toxic (El-Agnaf et al., 1998). Alternatively, in relation to its normal function, we must consider the possibility that synuclein may participate directly in cell death processes. Evidence in cell lines suggests that it does (Ostrerova et al., 1999). Our models provide an opportunity to examine directly in vivo the role of synuclein in an important form of cell death, apoptosis, in dopaminergic neurons of the SN, the neurons that degenerate in Parkinson's disease. In these models of apoptosis, the evidence we present suggests that synuclein is not playing a direct role in mediating death. On the contrary, our findings suggest that synuclein may normally play a role in compensatory or plasticity responses in surviving neurons. This observation suggests that perhaps it is loss or impairment of this function that mediates disease. Such a possibility is supported by the observation that synuclein mRNA content is reduced in the SN of Parkinson's patients at postmortem, more so than dopaminergic markers (Neystat et al., 1999). To test this hypothesis, it will be important in future studies to examine in synuclein null animals the sensitivity of dopamine neurons to neurotoxins that induce models of parkinsonism.

Acknowledgment: This work was supported by grant NS26836 from the National Institute of Neurological Disorders and Stroke (to R.E.B.), Shannon Award 07418 from the National Institute on Drug Abuse (to D.S.), grant 10154 from the National Institute on Drug Abuse (to D.S.), the Parkinson's Disease Foundation, the Lowenstein Foundation, the Smart Family Foundation, and the National Parkinson's Disease Foundation (to K.E.L.). We are grateful to Ms. Pat White for secretarial assistance. We are also grateful to Ms. M. Sundsmo of the laboratory of Dr. T. Saitoh for providing the anti-NACP and anti-NAC antibodies and to Dr. S. Hirose for supplying the antibody to transglutaminase. We are grateful to Drs. R. Scheller and S. Przedborski for their review of the manuscript, to Dr. L. Haynes for discussions of transglutaminase staining, and to Dr. K. Wilhelmsen for advice on differential display. We are grateful to Ms. Viviana Davila for assistance with single cell isolation, and to Dr. Przedborski for assistance with immunofluorescence double labeling.

REFERENCES

Altschul S. F., Gish W., Miller W., Myers E. W., and Lipman D. J. (1990) Basic local alignment search tool. *J. Mol. Biol.* **215,** 403–410.

Arawaka S., Saito Y., Murayama S., and Mori H. (1998) Lewy body in neurodegeneration with brain iron accumulation type 1 is immunoreactive for alpha-synuclein. *Neurology* **51,** 887–889.

Burke R. E., Macaya A., DeVivo D., Kenyon N., and Janec E. M. (1992) Neonatal hypoxic–ischemic or excitotoxic striatal injury results in a decreased adult number of substantia nigra neurons. *Neuroscience* **50,** 559–569.

Burke R. E., Franklin S. O., and Inturrisi C. E. (1994) Acute and persistent suppression of preproenkephalin mRNA expression in the striatum following developmental hypoxic–ischemic injury. *J. Neurochem.* **62,** 1878–1886.

Burke R. E., Antonelli M., and Sulzer D. (1998) Glial cell line-derived neurotrophic growth factor inhibits apoptotic death of postnatal substantia nigra dopamine neurons in primary culture. *J. Neurochem.* **71,** 517–525.

Clarke P. G. H. (1985) Neuronal death in the development of the vertebrate nervous system. *Trends Neurosci.* **8,** 345–349.

Clayton D. F. and George J. M. (1998) The synucleins: a family of proteins involved in synaptic function, plasticity, neurodegeneration and disease. *Trends Neurosci.* **21,** 249–254.

Colley W. C., Sung T. C., Roll R., Jenco J., Hammond S. M., Altshuller Y., Bar-Sagi D., Morris A. J., and Frohman M. A. (1997) Phospholipase D2, a distinct phospholipase D isoform with novel regulatory properties that provokes cytoskeletal reorganization. *Curr. Biol.* **7,** 191–201.

Coyle J. T. (1977) Biochemical aspects of neurotransmission in the developing brain. *Int. Rev. Neurobiol.* **20,** 65–102.

El-Agnaf O. M., Jakes R., Curran M. D., Middleton D., Ingenito R., Bianchi E., Pessi A., Neill D., and Wallace A. (1998) Aggregates from mutant and wild-type alpha-synuclein proteins and NAC peptide induce apoptotic cell death in human neuroblastoma cells by formation of beta-sheet and amyloid-like filaments. *FEBS Lett.* **440,** 71–75.

Estus S., Zaks W. J., Freeman R. S., Gruda M., Bravo R., and Johnson E. M. (1994) Altered gene expression in neurons during programmed cell death: identification of c-jun as necessary for neuronal apoptosis. *J. Cell Biol.* **127,** 1717–1727.

Fesus L., Davies P. J. A., and Piacentini M. (1991) Apoptosis: molecular mechanisms in programmed cell death. *Eur. J. Cell Biol.* **56,** 170–177.

George J. M., Jin H., Woods W. S., and Clayton D. F. (1995) Characterization of a novel protein regulated during the critical period for song learning in the zebra finch. *Neuron* **15,** 361–372.

Han H., Weinreb P. H., and Lansbury P. T. J. (1995) The core Alzheimer's peptide NAC forms amyloid fibrils which seed and are seeded by beta-amyloid: is NAC a common trigger or target in neurodegenerative disease? *Chem. Biol.* **2,** 163–169.

Hashimoto M., Hsu L. J., Sisk A., Xia Y., Takeda A., Sundsmo M., and Masliah E. (1998) Human recombinant NACP/alpha-synuclein is aggregated and fibrillated in vitro: relevance for Lewy body disease. *Brain Res.* **799,** 301–306.

Irizarry M. C., Kim T. W., McNamara M., Tanzi R. E., George J. M., Clayton D. F., and Hyman B. T. (1996) Characterization of the precursor protein of the non-A beta component of senile plaques (NACP) in the human central nervous system. *J. Neuropathol. Exp. Neurol.* **55,** 889–895.

Iwai A., Masliah E., Yoshimoto M., Ge N., Flanagan L., de Silva H. A. R., Kittel A., and Saitoh T. (1995*a*) The precursor protein of non-Aβ component of Alzheimer's disease amyloid is a presynaptic protein of the central nervous system. *Neuron* **14,** 467–475.

Iwai A., Yoshimoto M., Masliah E., and Saitoh T. (1995*b*) Non-Aβ component of Alzheimer's disease amyloid (NAC) is amyloidogenic. *Biochemistry* **34,** 10139–10145.

Jakes R., Spillantini M. G., and Goedert M. (1994) Identification of two distinct synucleins from human brain. *FEBS Lett.* **345,** 27–32.

Janec E. and Burke R. E. (1993) Naturally occurring cell death during postnatal development of the substantia nigra of the rat. *Mol. Cell. Neurosci.* **4,** 30–35.

Jenco J. M., Rawlingson A., Daniels B., and Morris A. J. (1998) Regulation of phospholipase D2: selective inhibition of mammalian phospholipase D isoenzymes by alpha- and beta-synucleins. *Biochemistry* **37,** 4901–4909.

Jensen P. H., Sorensen E. S., Petersen T. E., Gliemann J., and Rasmussen L. K. (1995) Residues in the synuclein consensus motif of the α-synuclein fragment, NAC, participate in transglutaminase-catalysed cross-linking to Alzheimer-disease amyloid βA4 peptide. *Biochem. J.* **310,** 91–94.

Jeon B. S., Kholodilov N. G., Oo T. F., Kim S.-Y., Tomaselli K. J., Srinivasan A., Stefanis L., and Burke R. E. (1999) Activation of caspase-3 in developmental models of programmed cell death in neurons of the substantia nigra. *J. Neurochem.* **73,** 322–333.

Ji H., Liu Y. E., Jia T., Wang M., Liu J., Xiao G., Joseph B. K., Rosen C., and Shi Y. E. (1997) Identification of a breast cancer-specific gene, BCSG1, by direct differential cDNA sequencing. *Cancer Res.* **57,** 759–764.

Kelly W. J. and Burke R. E. (1996) Apoptotic neuron death in rat substantia nigra induced by striatal excitotoxic injury is developmentally dependent. *Neurosci. Lett.* **220,** 85–88.

Kholodilov N. G., Neystat M., and Burke R. E. (1997) Investigation of apoptotic neuron death in substantia nigra with mRNA differential display. (Abstr.) *Neurology* **48,** A322.

Kholodilov N. G., Oo T. F., and Burke R. E. (1999) Synuclein expression is decreased in rat substantia nigra following induction of apoptosis by intrastriatal 6-hydroxydopamine. *Neurosci. Lett.* (in press).

Kruger R., Kuhn W., Muller T., Woitalla D., Graeber M., Kosel S., Przuntek H., Epplen J. T., Schols L., and Riess O. (1998) Ala30Pro mutation in the gene encoding alpha-synuclein in Parkinson's disease. *Nat. Genet.* **18,** 106–108.

Lavedan C. (1998) The synuclein family. *Genome Res.* **8,** 871–880.

Lavedan C., Leroy E., Dehejia A., Buchholtz S., Dutra A., Nussbaum R. L., and Polymeropoulos M. H. (1998) Identification, localization and characterization of the human gamma-synuclein gene. *Hum. Genet.* **103,** 106–112.

Macaya A., Munell F., Gubits R. M., and Burke R. E. (1994) Apoptosis in substantia nigra following developmental striatal excitotoxic injury. *Proc. Natl. Acad. Sci. USA* **91,** 8117–8121.

Mackay D. J. G., Nobes C. D., and Hall A. (1995) The Rho's progress: a potential role during neuritogenesis for the Rho family of GTPases. *Trends Neurosci.* **18,** 496–501.

Maroteaux L. and Scheller R. H. (1991) The rat brain synucleins; family of proteins transiently associated with neuronal membrane. *Mol. Brain Res.* **11,** 335–343.

Maroteaux L., Campanelli J. T., and Scheller R. H. (1988) Synuclein: a neuron-specific protein localized to the nucleus and presynaptic nerve terminal. *J. Neurosci.* **8,** 2804–2815.

Marti M. J., James C. J., Oo T. F., Kelly W. J., and Burke R. E. (1997) Early developmental destruction of terminals in the striatal target induces apoptosis in dopamine neurons of the substantia nigra. *J. Neurosci.* **17,** 2030–2039.

Mena M. A., Davila V., and Sulzer D. (1997) Neurotrophic effects of L-DOPA in postnatal midbrain dopamine neuron/cortical astrocyte cocultures. *J. Neurochem.* **69,** 1398–1408.

Mochizuki H., Goto K., Mori H., and Mizuno Y. (1996) Histochemical detection of apoptosis in Parkinson's disease. *J. Neurol. Sci.* **137,** 120–123.

Morgan J. I. and Curran T. (1995) The immediate-early gene response and neuronal death and regeneration. *Neuroscientist* **1,** 68–75.

Nakajo S., Tsukada K., Omata K., Nakamura Y., and Nakaya K. (1993) A new brain-specific 14-kDa protein is a phosphoprotein. Its complete amino acid sequence and evidence for phosphorylation. *Eur. J. Biochem.* **217,** 1057–1063.

Nakajo S., Shioda S., Nakai Y., and Nakaya K. (1994) Localization of phosphoneuroprotein 14 (PNP 14) and its mRNA expression in rat brain determined by immunocytochemistry and in situ hybridization. *Mol. Brain Res.* **27,** 81–86.

Neystat M., Lynch T., Przedborski S., Kholodilov N. G., Rzhetskaya M., and Burke R. E. (1999) Alpha-synuclein expression in substantia nigra and cortex in Parkinson's disease. *Mov. Disord.* **14,** 417–422.

Oo T. F. and Burke R. E. (1997) The time course of developmental cell death in phenotypically defined dopaminergic neurons of the substantia nigra. *Dev. Brain Res.* **98,** 191–196.

Oo T. F., Henchcliffe C., James D., and Burke R. E. (1999) Expression of c-fos, c-jun, and c-jun N-terminal kinase (JNK) in a developmental model of induced apoptotic death in neurons of the substantia nigra. *J. Neurochem.* **72,** 557–564.

Ostrerova N., Petrucelli L., Farrer M., Mehta N., Choi P., Hardy J., and Wolozin B. (1999) Alpha-synuclein shares physical and functional homology with 14-3-3 proteins. *J. Neurosci.* **19,** 5782–5791.

Paxinos G. and Watson C. (1982) *The Rat Brain in Stereotaxic Coordinates.* Academic Press, San Diego.

Perry M. J. M. and Haynes L. W. (1993) Localization and activity of transglutaminase, a retinoid-inducible protein, in developing rat spinal cord. *Int. J. Dev. Neurosci.* **11,** 325–337.

Petersen K., Olesen O. F., and Mikkelsen J. D. (1999) Developmental expression of alpha-synuclein in rat hippocampus and cerebral cortex. *Neuroscience* **91,** 651–659.

Phillips J. and Eberwine J. H. (1996) Antisense RNA amplification: a linear amplification method for analyzing the mRNA population from single living cells. *Methods* **10,** 283–288.

Polymeropoulos M. H., Lavedan C., Leroy E., Ide S. E., Dehejia A., Dutra A., Pike B., Root H., Rubenstein J., Boyer R., Stenroos E. S., Chandrasekharappa S., Athanassiadou A., Papapetropoulos T., Johnson W. G., Lazzarini A. M., Duvoisin R. C., Golbe L. I., and Nussbaum R. L. (1997) Mutation in the α-synuclein gene identified in families with Parkinson's disease. *Science* **276,** 2045–2047.

Pothos E. N., Davila V., and Sulzer D. (1998) Presynaptic recording of quanta from midbrain dopamine neurons and modulation of the quantal size. *J. Neurosci.* **18,** 4106–4118.

Przedborski S., Khan U., Kostic V., Carlson E., Epstein C. J., and Sulzer D. (1996) Increased superoxide dismutase activity improves survival of cultured postnatal midbrain neurons. *J. Neurochem.* **67,** 1383–1392.

Rayport S., Sulzer D., Shi W. X., Sawasdikosol S., Monaco J., Batson D., and Rajendran G. (1992) Identified postnatal mesolimbic dopamine neurons in culture: morphology and electrophysiology. *J. Neurosci.* **12,** 4264–4280.

Spillantini M. G., Schmidt M. L., Lee V. M. Y., Trojanowski J. Q., Jakes R., and Goedert M. (1997) α-Synuclein in Lewy bodies. *Nature* **388,** 839–840.

Sulzer D., Maidment N. T., and Rayport S. (1993) Amphetamine and other weak bases act to promote reverse transport of dopamine in ventral midbrain neurons. *J. Neurochem.* **60,** 527–535.

Surguchov A., Surgucheva I., Solessio E., and Baehr W. (1999) Synoretin—a new protein belonging to the synuclein family. *Mol. Cell. Neurosci.* **13,** 95–103.

Tompkins M. M., Basgall E. J., Zamrini E., and Hill W. D. (1997) Apoptotic-like changes in Lewy-body-associated disorders and normal aging in substantia nigral neurons. *Am. J. Pathol.* **150,** 119–131.

Tu P. H., Galvin J. E., Baba M., Giasson B., Tomita T., Leight S., Nakajo S., Iwatsubo T., Trojanowski J. Q., and Lee V. M. (1998) Glial cytoplasmic inclusions in white matter oligodendrocytes of multiple system atrophy brains contain insoluble alpha-synuclein. *Ann. Neurol.* **44,** 415–422.

Ueda K., Fukushima H., Masliah E., Xia Y., Iwai A., Yoshimoto M., Otero D. A. C., Kondo J., Ihara Y., and Saitoh T. (1993) Molecular cloning of cDNA encoding an unrecognized component of amyloid in Alzheimer disease. *Proc. Natl. Acad. Sci. USA* **90,** 11282–11286.

Withers G. S., George J. M., Banker G. A., and Clayton D. F. (1997) Delayed localization of synelfin (synuclein, NACP) to presynaptic terminals in cultured rat hippocampal neurons. *Dev. Brain Res.* **99,** 87–94.